MODELLING ANTENNAS IN OUTER SPACE USING THE BOUNDARY ELEMENT UNSTRUCTURED TRANSMISSION-LINE (BEUT) METHOD

Daniel Simmons, Kristof Cools, and Phil Sewell

George Green Institute for Electromagnetics Research, University of Nottingham, U.K.

ABSTRACT

In this paper the hybridization of the 2D time domain boundary element method (BEM) with the unstructured transmission line method (UTLM) is described. The novel method enables accurate modelling of radiating boundary conditions, excitation by plane waves, and efficient modelling of problems containing large free-space regions and non-uniform materials. The method has been developed to more accurately describe arbitrary surfaces and is demonstrated by comparing numerical results against analytical results.

Key words: UTLM; BEM; BEUT; hybrid .

1. INTRODUCTION

Modelling transient electromagnetic fields in space-science applications is difficult because of the large radiation environment and the presence of potentially complex geometries with non-uniform material parameters. These demanding circumstances require a mix of volume and surface discretizing numerical techniques to accurately and efficiently simulate the problem.

The transmission line modelling (TLM) technique is a popular space discretizing method which maps a passive electrical circuit to the field problem, meaning it is explicitly stable and conservative (Christopoulos 1995). The unstructured TLM (UTLM) enables meshing with triangles or tetrahedra removing some of the initial drawback of the algorithm such as the need to use structured meshing tools and the presence of staircasing. This means that complex geometrical shapes with curved surfaces can be more accurately discretized by providing piecewise linear boundary descriptions (Nasser et al. 2015).

The boundary element method (BEM) solves the integral form of Maxwell's equations for field components on the surface of objects. Like all surface based numerical methods, it can deal with large free space regions using just the boundaries, thus it reduces the the complexity of the problem by one dimension. The technique is also implicitly causal and has excellent radiation conditions.

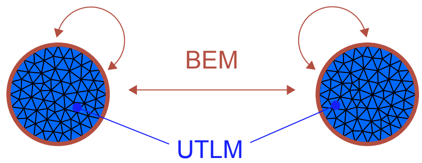

Figure 1. Arbitrary objects modelled using UTLM, separated by free space modelled by BEM.

The time domain BEM requires knowledge of the time domain green function and the resulting linear system is solved using the marching-on-in-time algorithm.

The advantages of hybridizing UTLM and BEM include:

- Ability to model geometrically complex, inhomogeneous objects
- Accurate simulation of radiating boundary conditions
- Straightforward excitation of plane waves, useful for computing radar cross sections, and notoriously difficult to implement in a pure TLM setting
- Efficient computation of scattering problems where free space dominates, a feature of BEM solvers that now also becomes available in the presence of non-uniform media

Previous hybrid BEM and TLM methods have been developed, for the case of Cartesian TLM, by Pierantoni et al. (1997); Lindenmeier et al. (1998, 1999a,b, 2000); Zedler & Eleftheriades (2011). However, these techniques do not consider the more flexible unstructured TLM algorithm, or recent advancements in BEM that make it more accurate and stable. The methodology used in this work is also conceptually very simple, and does not require transitional padding layers or the use of discrete Green's functions.

Our hybridization of the time domain BEM and UTLM techniques is called the boundary element unstructured transmission-line (BEUT) method. The aim of this paper is to explain the theory behind this novel method, and then how it is implemented. It will be demonstrated using a canonical test case analysing the frequency response of a dielectric cylinder and comparisons made between pure UTLM, BEUT, and analytical solutions.

2. INTRODUCTION TO THE HYBRID METHOD

We will consider a 2D domain in which two arbitrary objects are separated by an arbitrary distance in free space as shown in Figure 1. Each object may have complex material parameters modelled using triangles, with each triangle representing the material parameter of its discretized region as stipulated in the UTLM method described by Sewell et al. (2004). The field inside each triangle will be modelled using electrical transmission lines excited by pulses originating from neighbouring triangles at a previous time step. The free space region will not be meshed; Instead the BEM method will deduce the fields on the boundaries at the current timestep using the interactions between the fields at every boundary edge, including all those that occurred previously in time.

To keep this contribution self-contained, the recently introduced BEUT method by Simmons et al. (2015) for the coupling of UTLM and BEM will be briefly revisited.

2.1. BEM

The BEM method is constructed starting from the time domain representation formulas. The representation formulas for the 2D transverse magnetic (TM) case are in structure very similar to those in the full 3D case as described in by Beghein et al. (2012), and can be written as

$$\begin{pmatrix} e_z \\ h_t \end{pmatrix} = \begin{pmatrix} \frac{1}{2} + D & -\frac{\eta}{c} S \\ -\frac{c}{\eta} N & \frac{1}{2} - D' \end{pmatrix} \begin{pmatrix} e_z \\ h_t \end{pmatrix} + \begin{pmatrix} e_z^i \\ h_t^i \end{pmatrix} \quad (1)$$

where the characteristic impedance is $\eta = \sqrt{\mu/\epsilon}$ and the wave propagation speed is $c = \sqrt{\mu\epsilon}$. e_z and h_t denote the tangential components of the electric and magnetic fields respectively, and superscript i denotes an incident field. The operators in equation 1 can be defined as

$$D\varphi(\boldsymbol{\rho}', t) = \int_\Gamma \frac{\partial g(P,t)}{\partial n'} * \varphi(\boldsymbol{\rho}', t)\, d\rho'$$

$$D'\varphi(\boldsymbol{\rho}', t) = \int_\Gamma \frac{\partial g(P,t)}{\partial n} * \varphi(\boldsymbol{\rho}', t)\, d\rho'$$

$$S\varphi(\boldsymbol{\rho}', t) = \int_\Gamma g(P,t) * \frac{\partial}{\partial t}\varphi(\boldsymbol{\rho}', t)\, d\rho'$$

$$N\varphi(\boldsymbol{\rho}', t) = -\int_t \int_\Gamma \frac{\partial^2 g(P,t)}{\partial n\, \partial n'} * \varphi(\boldsymbol{\rho}', t)\, dn'\, dt$$

where t is the time, Γ is the object boundary, $*$ indicates a temporal convolution, and $P = |\boldsymbol{\rho} - \boldsymbol{\rho}'|$. The 2D time domain Green's function is defined as the field radiated by a Dirac source, represented here as

$$g(P,t) = \frac{H(t - P/c)}{2\pi\sqrt{t^2 - (P/c)^2}}$$

where H denotes the Heaviside function.

The implementation of the above formulation will be discussed in section 3.

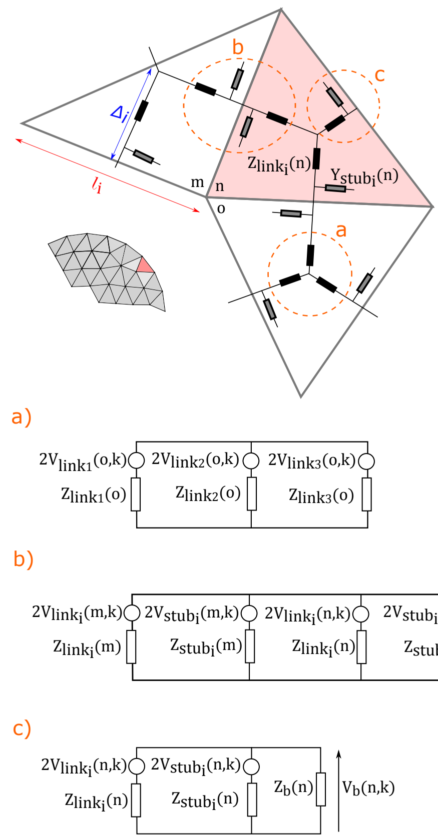

Figure 2. The transmission lines inside UTLM triangles along with Thevénin equivalent circuits at timestep, k, for a) scattering, b) connection between triangles, and c) connection at the boundaries.

2.2. Unstructured TLM

The 2D UTLM method maps temporal electric and magnetic fields to voltages and currents which travel in transmission lines normal to the edges of triangles in an unstructured mesh (Sewell et al. 2004).

A generic UTLM triangle is shown in Figure 2. Local material parameters are modelled with transmission lines (a.k.a. link lines) which connect every triangle circumcenter through ports. Each link line has an associated impedance, Z_{link}, which is related to its admittance using $Z_{\text{link}} = 1/Y_{\text{link}}$. Additional stubs, which are transmission lines terminated by an open circuit, are used for more accurate modelling. Each stub has an associated admittance, Y_{stub}.

We can simulate transverse magnetic fields using a shunt mode configuration, where the appropriate link and stub admittances are defined as

$$Y_{\text{link}_i} = \frac{l_i \Delta t}{2\mu\Delta_i}$$
$$Y_{\text{stub}_i} = \frac{\epsilon l_i \Delta_i}{\Delta t} - \frac{l_i \Delta t}{2\mu\Delta_i}$$

The relative triangle port is denoted by subscript i, the link length is denoted by Δ_i, and the edge length is given by l_i. The permeability and permittivity of the medium is denoted by μ and ϵ respectively.

The UTLM method operates by subsequent calculation of the response of the transmission line network using the signal obtained at the previous timestep in adjacent cells, which can be analytically shown to be conservative. It is implemented in a time loop which consists of 3 main stages for each timestep:

1. Scatter - compute the reflected signals using the incoming signals at each triangle circumcenter
2. Connect between triangles - use the reflected signals to compute the signals that are to be incident in the next timestep, including any point source excitations
3. Connect at the boundaries - compute the signals coming from the boundary edges using the reflected signals incident to the boundary and a suitable boundary condition

This process is depicted in Figure 2, along with the Thevénin equivalent circuit diagrams for each stage. Simple nodal analysis can be used to find incident and reflected voltages. This demonstrates the educational appeal of TLM, as its workings can be made plausible using concepts that are available at an early stage in a classic electrical engineering programme.

2.3. BEUT

The hybridization of BEM and UTLM is achieved by enforcing continuity conditions at the interface between the object and free space. Traditionally, to model a radiating boundary, the UTLM boundary impedance is set to be proportional to the characteristic impedance of free space. This reduces the radiation problem locally to a one dimensional transmission problem. Even though this approach has been proven to be partially successful, it is an approximation and introduces error, especially in the presence of obliquely incident fields and at non-smooth regions in the interface.

BEUT does not suffer from the aforementioned drawbacks as we now replace the local boundary impedance with an interaction matrix which couples all interface edges, as defined in equation 1. This can be thought of as replacing the exterior region with a gigantic TLM cell which has an internal memory stretching back in time, resulting in a convolution over all previous time steps. This is as opposed to the retrieval of just the last timestep as with normal TLM cells.

The combination of link line and stub at a boundary can be replaced by a single impedance and voltage source by computation of the Thevénin equivalent. This network in turn can be seen to be the Thevénin equivalent of a single transmission line network, giving rise to the following 1D representation theorem, valid for voltage/current pairs on the UTLM/BEM boundaries

$$\begin{pmatrix} V_b \\ I_b \end{pmatrix} = \begin{pmatrix} \frac{1}{2} & \frac{Z_{\text{total}}}{2} \\ \frac{Y_{\text{total}}}{2} & \frac{1}{2} \end{pmatrix} \begin{pmatrix} V_b \\ I_b \end{pmatrix} + \begin{pmatrix} \frac{V_{\text{open}}}{2} \\ -\frac{I_{\text{closed}}}{2} \end{pmatrix} \tag{2}$$

$$I_{\text{closed}} = 2V^{\text{r}}_{\text{link}} Y_{\text{link}} + 2V^{\text{r}}_{\text{stub}} Y_{\text{stub}} \tag{3}$$

$$V_{\text{open}} = \frac{I_{\text{closed}}}{Y_{\text{total}}} \tag{4}$$

where the matrices Y_{total} and Z_{total} are diagonal, and $Y_{\text{total}} = Y_{\text{link}} + Y_{\text{stub}}$.

The mapping between voltages and currents with tangential electric and magnetics fields, respectively, is governed by the following equivalences

$$e_{\text{z}} \leftrightarrow V_b \qquad h_{\text{t}} l_b \leftrightarrow I_b \tag{5}$$

where l_b denotes the edge length at boundary edge b.

Using these equivalences, we can combine the representation formulas 1 and 2 to obtain the following convolution equation for the boundary unknowns

$$\begin{pmatrix} e^{\text{i}}_{\text{z}} \\ h^{\text{i}}_{\text{t}} l_b \end{pmatrix} + \frac{1}{2} \begin{pmatrix} -V_{\text{open}} \\ I_{\text{closed}} \end{pmatrix} = \begin{pmatrix} -D & \frac{Z_{\text{total}}}{2} + \frac{\eta}{c} S {l_b}^{-1} \\ \frac{Y_{\text{total}}}{2} + \frac{c}{\eta} N l_b & D' \end{pmatrix} \begin{pmatrix} V_b \\ I_b \end{pmatrix} \tag{6}$$

The first term represents an exterior incident field contribution, the second term represents the transmission line signals incident on the boundary, and the third term is the interaction matrix which relates voltage and current but also takes into account the immediate impedance and all previous interactions.

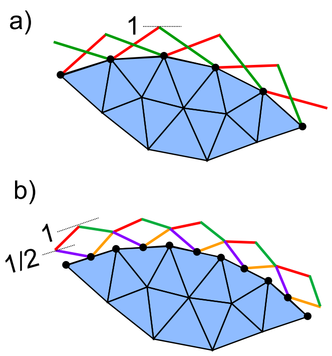

Figure 3. The boundary section of a scatterer with a) hat functions, and b) dual hat functions.

3. IMPLEMENTATION OF THE BEUT METHOD

To ensure continuity of the tangential magnetic field in the UTLM method, triangular meshes must be Delaunay as explained by Sewell et al. (2004). This means that link lines will travel between triangle circumcenters through the midpoints of each edge of a triangle.

When considering implementation of a numerical modelling tool for arbitrary objects, the unknown fields must be discretized using a combination of spatial and temporal basis functions. UTLM implicitly uses piecewise constant basis functions defined on the triangle edges. However, because of the derivatives found in the N operator, BEM has to use at least piecewise polynomial basis and test functions. Test functions are used because the Green's function must be integrated over source *and* observation points, and are equal to the basis functions which is a rule stipulated by the Galerkin method. The Lagrange interpolator is used for the temporal basis functions, and a collocation-in-time testing scheme is used.

Because of the need for piecewise polynomial spatial basis functions, hat functions are used as shown in Figure 3a. However, the degrees of freedom corresponding to these basis functions are located at the vertices. To reconcile the UTLM and BEM degrees of freedom, dual basis functions as shown in Figure 3b will be used in the BEM method. These basis functions are both sufficiently smooth and have degrees of freedoms attached to the edges as opposed to the vertices (Cools 2012).

To minimise dispersion error in UTLM, every stub admittance must have a positive value, thus the timestep, $\Delta t < \triangle_{i_{\text{min}}} \sqrt{2\mu\epsilon}$. Since this is likely to be small, the BEM temporal convolutions in equation 1 must be carefully integrated, especially near the Green's function singularities.

The BEUT workflow for every timestep is the same as with UTLM, but between scatter and connect stages, the BEUT equation 6 is solved to obtain updated boundary values, which are then used for connection at the boundaries.

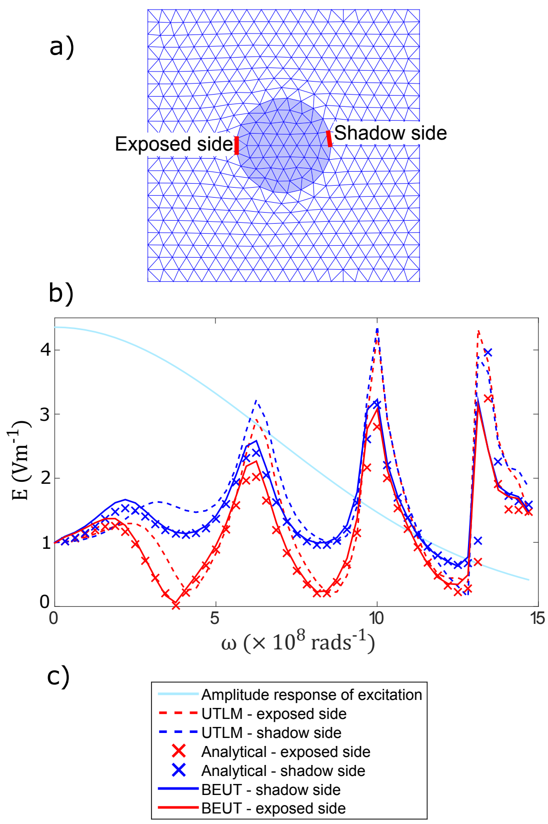

Figure 4. Results comparing BEUT with pure UTLM and analytic solutions when modelling a dielectric cylinder. The figure shows a) the mesh, b) the plot of results, and c) the legend.

4. RESULTS

We excite a 2D dielectric cylinder with a plane wave as shown in Figure 4a. After monitoring the electric field at the surface at the exposed side (boundary edge nearest to the excitation source) and shadow side (boundary edge furthest from the excitation source) for a sufficient time, we compute the Fourier transform. There is an analytical solution to this problem in the frequency domain as as can be found in for example in Jin (2011). This solution is compared against using purely UTLM, and then using the BEUT method.

Modelling plane waves in TLM can be found for example in Zedler & Eleftheriades (2011) and Khashan et al. (2015). The boundaries normal to the angle of incidence are terminated with matched boundaries, and the boundaries tangential to the angle of incidence are terminated with open circuits. However, these boundary conditions are only accurate for the incident field, hence our UTLM model updates the boundaries once the scattered field is detected.

The results are compared in Figure 4. The frequency response using the BEUT method more closely matches the analytic results than the corresponding UTLM method. Of course, the areas of mesh representing free space are no longer needed if the BEUT method is used, so we can simply use the inner cylindrical mesh to get more accurate results, and with less computational resources.

This is a simple canonical test case, but there is enormous scope for the BEUT method. The accurate response due to radiation from multiple satellites at far distances away can now be modelled without needing to mesh the free space in between. Recent advances in TLM also allow it to model materials with frequency dependant properties (Paul et al. 1999), which would be useful for measuring the effects of solar wind, and spacecraft charging.

5. CONCLUSION

The hybrid BEUT method theory and notes on its implementation has been described. Field vectors were expanded using dual basis functions to satisfy spatial continuity at the boundaries, and results were obtained which showed good agreement with analytic solutions.

There are many advantages of hybridizing UTLM and BEM, including perfect radiating boundaries and the ability to efficiently solve scattering problems where free space dominates. This makes it an invaluable tool for modelling electromagnetic fields in outer space due to the presence of complex media and the abundance of free space.

REFERENCES

Beghein, Y., Cools, K., Andriulli, F. P., De Zutter, D., & Michielssen, E. 2012, IEEE Trans. Antennas Propag., 60, 4239

Christopoulos, C. 1995, The Transmission-Line Modeling Method TLM, The IEEE Series on Electromagnetic Wave Theory (Wiley)

Cools, K. 2012, cccc2012 Asia-Pacific Symp. Electromagn. Compat. APEMC 2012 - Proc., 165

Jin, J.-M. J. 2011, Theory and Computation of Electromagnetic Fields, ed. I. PRESS (John Wiley & Sons)

Khashan, L., Vukovic, A., Sewell, P., & Benson, T. M. 2015, in 2015 IEEE Int. Conf. Comput. Electromagn. (IEEE), 347–349

Lindenmeier, S., Christopoulos, C., & Russer, P. 2000, 2000 IEEE MTT-S Int. Microw. Symp. Dig. (Cat. No.00CH37017), 1, 387

Lindenmeier, S., Pierantoni, L., & Russer, P. 1998, 1998 IEEE MTT-S Int. Microw. Symp. Dig. (Cat. No.98CH36192), 2, 465

Lindenmeier, S., Pierantoni, L., & Russer, P. 1999a, IEEE Trans. Electromagn. Compat., 41, 425

Lindenmeier, S., Pierantoni, L., & Russer, P. 1999b, Int. J. Numer. Model. Electron. Networks, Devices Fields, 12, 295

Nasser, H., Greedy, S., Benson, T., Vukovic, A., & Sewell, P. 2015, in 2015 IEEE Int. Conf. Comput. Electromagn. No. 4822 (IEEE), 338–340

Paul, J., Christopoulos, C., & Thomas, D. 1999, IEEE Trans. Antennas Propag., 47, 1528

Pierantoni, L., Lindenmeier, S., & Russer, P. 1997, 27th Eur. Microw. Conf. 1997, 2, 937

Sewell, P., Wykes, J., Benson, T., et al. 2004, IEEE Trans. Microw. Theory Tech., 52, 1490

Simmons, D., Cools, K., & Sewell, P. 2015, in ICEAA (Torino: (submitted for publication))

Zedler, M. & Eleftheriades, G. V. 2011, Proc. IEEE, 99, 1634